Mitochondrial ATP-sensitive K^+ channels regulate NMDAR activity in the cortex of the anoxic western painted turtle

Matthew Edward Pamenter[1,2], Damian Seung-Ho Shin[3], Mohan Cooray[1] and Leslie Thomas Buck[1,2]

[1]*Department of Cellular and Systems Biology, University of Toronto, Toronto, ON, Canada M5S 3G5*
[2]*Department of Ecology and Evolutionary Biology, University of Toronto, Toronto, ON, Canada M5S 3G5*
[3]*Division of Fundamental Neurobiology, Toronto Western Research Institute, Toronto, ON, Canada M5T 2S8*

Hypoxic mammalian neurons undergo excitotoxic cell death, whereas painted turtle neurons survive prolonged anoxia without apparent injury. Anoxic survival is possibly mediated by a decrease in *N*-methyl-D-aspartate receptor (NMDAR) activity and maintenance of cellular calcium concentrations ($[Ca^{2+}]_c$) within a narrow range during anoxia. In mammalian ischaemic models, activation of mitochondrial ATP-sensitive K^+ (mK_{ATP}) channels partially uncouples mitochondria resulting in a moderate increase in $[Ca^{2+}]_c$ and neuroprotection. The aim of this study was to determine the role of mK_{ATP} channels in anoxic turtle NMDAR regulation and if mitochondrial uncoupling and $[Ca^{2+}]_c$ changes underlie this regulation. In isolated mitochondria, the K_{ATP} channel activators diazoxide and levcromakalim increased mitochondrial respiration and decreased ATP production rates, indicating mitochondria were 'mildly' uncoupled by 10–20%. These changes were blocked by the mK_{ATP} antagonist 5-hydroxydecanoic acid (5HD). During anoxia, $[Ca^{2+}]_c$ increased $9.3 \pm 0.3\%$ and NMDAR currents decreased $48.9 \pm 4.1\%$. These changes were abolished by K_{ATP} channel blockade with 5HD or glibenclamide, Ca_c^{2+} chelation with 1,2-bis(*o*-aminophenoxy)ethane-*N*,*N*,*N*′,*N*′-tetraacetic acid (BAPTA) or by activation of the mitochondrial Ca^{2+} uniporter with spermine. Similar to anoxia, diazoxide or levcromakalim increased $[Ca^{2+}]_c$ $8.9 \pm 0.7\%$ and $3.8 \pm 0.3\%$, while decreasing normoxic whole-cell NMDAR currents by $41.1 \pm 6.7\%$ and $55.4 \pm 10.2\%$, respectively. These changes were also blocked by 5HD or glibenclamide, BAPTA, or spermine. Blockade of mitochondrial Ca^{2+}-uptake decreased normoxic NMDAR currents $47.0 \pm 3.1\%$ and this change was blocked by BAPTA but not by 5HD. Taken together, these data suggest mK_{ATP} channel activation in the anoxic turtle cortex uncouples mitochondria and reduces mitochondrial Ca^{2+} uptake via the uniporter, subsequently increasing $[Ca^{2+}]_c$ and decreasing NMDAR activity.

(Received 2 August 2007; accepted after revision 12 December 2007; first published online 13 December 2007)
Corresponding author L.T. Buck: University of Toronto, Dept. of Cellular and Systems Biology, 25 Harbord Street, Toronto, ON M5S 3G5. buckl@zoo.utoronto.ca

When mammalian brain experiences ischaemia, excessive glutamate release triggers massive Ca^{2+} influx through *N*-methyl-D-aspartate receptors (NMDARs), leading to excitotoxic cell death (ECD) (Choi, 1992; Zipfel *et al.* 2000). Blockade of NMDARs is neuroprotective of focal ischaemia in animal models (Arundine & Tymianski, 2003) but results in deleterious side-effects in clinical trials (Ikonomidou & Turski, 2002). An alternative to NMDAR blockade is up-stream modulation of receptor activity via endogenous mechanisms. In the cerebral cortex of the painted turtle (*Chrysemys picta belli*) NMDAR activity decreases up to 65% during anoxia while neuronal activity is preserved (Buck & Bickler, 1995; Buck & Bickler, 1998; Bickler *et al.* 2000; Shin & Buck, 2003; Shin *et al.* 2005). This reduction in NMDAR activity occurs via an intracellular signalling mechanism and not through direct blockade of the NMDAR.

Although mammals exposed to anoxia suffer ECD, they can survive brief periods of ischaemia without serious impairment of neuronal function. In fact, tolerable ischaemic insults actually protect against subsequent longer duration insults in a mechanism of neuroprotection termed ischaemic preconditioning (IPC) (Murry *et al.* 1986). There is growing consensus that this protection is mediated by the partial uncoupling of mitochondria following the activation of mitochondrial ATP-sensitive potassium (mK_{ATP}) channels. In particular, evidence of mK_{ATP} channel-mediated neuroprotection has been shown in cultured rat cortical neurons exposed to glutamate toxicity (Kis *et al.* 2003, 2004); following

 DOI: 10.1113/jphysiol.2007.142380

cerebral artery occlusion in rats (Shimizu *et al.* 2002); in rat hippocampal and cortical neurons following anoxia/reperfusion injury (Heurteaux *et al.* 1995; Semenov *et al.* 2000); and in anoxic juvenile mouse brainstem (Muller *et al.* 2002).

One possible mechanism underlying mK_{ATP} channel-based neuroprotection is regulation of mitochondrial Ca^{2+} uptake and prevention of mitochondrial Ca^{2+} overload. Opening of mK_{ATP} channels increases mitochondrial K^+ conductance (mG_K), which is opposed by the mitochondrial K^+/H^+ exchanger, whose activation dissipates the mitochondrial proton gradient. This depolarization mildly uncouples the mitochondrial inner membrane potential (Holmuhamedov *et al.* 1999). This potential drives the Ca^{2+} uniporter and thus mitochondrial Ca^{2+} uptake. In rat cortical slices blockade of the Ca^{2+} uniporter decreases NMDAR activity and reduces glutamate-induced Ca^{2+} influx (Kannurpatti *et al.* 2000). Thus NMDAR activity has been linked to mitochondrial Ca^{2+} uptake and mK_{ATP} channels have been linked to the regulation of this uptake (Buck & Pamenter, 2006).

In the anoxic turtle cortex, $[Ca^{2+}]_c$ is moderately elevated, and large cytotoxic $[Ca^{2+}]_c$ increases observed in anoxic mammalian tissues are avoided. Paradoxically, this small increase in $[Ca^{2+}]_c$ attenuates turtle NMDAR activity and prevents larger lethal increases in $[Ca^{2+}]_c$ (Bickler *et al.* 2000). Similarly, a mild elevation in rat hippocampal $[Ca^{2+}]_c$ was neuroprotective against subsequent ischaemic insults, preventing toxic accumulation of $[Ca^{2+}]_c$ and reducing cell death (Bickler & Fahlman, 2004). We hypothesize that activation of mK_{ATP} channels impairs mitochondrial Ca^{2+} uptake, elevates $[Ca^{2+}]_c$ and attenuates NMDAR activity in the turtle cortex. The aims of this paper are to determine (1) whether mK_{ATP} channels are present in turtle mitochondria, (2) if activation of these channels uncouples mitochondria, (3) if mK_{ATP} channels can regulate NMDA receptor activity in the normoxic turtle cortex, (4) if mK_{ATP} channel activity underlies the anoxic decrease in NMDA receptor activity, and (5) whether effects of mK_{ATP} channel activity on NMDA receptor currents are Ca^{2+} dependent.

Methods

Ethics approval

This study was approved by the University of Toronto Animal Care committee and conforms to the *Guide to the Care and Use of Experimental Animals*, volume 2 as determined by the Canadian Council on Animal Care regarding relevant guidelines for the care of experimental animals. Adult turtles were obtained from Niles Biological Inc. (Sacramento, CA, USA).

Dissection and whole-cell patch-clamp recordings

All experiments were conducted at a room temperature of 22°C. Basic methods for turtle cortical sheet dissection and whole-cell patch-clamp techniques are described elsewhere (Shin & Buck, 2003). Briefly, turtles were decapitated and whole brains were rapidly excised from the cranium within 30 s of decapitation. Cortical sheets were isolated from the whole brain in artificial turtle cerebrospinal fluid (aCSF; mM: 107 NaCl, 2.6 KCl, 1.2 $CaCl_2$, 1 $MgCl_2$, 2 NaH_2PO_4, 26.5 $NaHCO_3$, 10 glucose, 5 imidazole, pH 7.4; osmolality 280–290 mosmol l^{-1}). For caesium experiments 1.2 mM $CsCl_2$ was substituted for $CaCl_2$. NMDAR currents are not inhibited by the concentration of Mg^{2+} used in these experiments (Shin & Buck, 2003).

Cortical sheets were placed in an RC-26 chamber with a P1 platform (Warner Instruments, CT, USA). The chamber was gravity perfused at a rate of 2–3 ml min^{-1}. Normoxic aCSF was gassed with 95% O_2–5% CO_2 and a second bottle with 95% N_2–5% CO_2 to achieve an anoxic perfusion. To maintain anoxic conditions, perfusion tubes from IV bottles were double jacketed and the outer jacket gassed with 95% N_2–5% CO_2. The anoxic aCSF reservoir was bubbled for 30 min before an experiment. A plastic cover with a hole for the recording electrode was placed over the perfusion chamber and the space between the fluid surface and cover was gently gassed with 95% N_2–5% CO_2. Throughout the entire anoxic experiment, aCSF was constantly gassed with N_2/CO_2. The partial pressure of oxygen (P_{O_2}) in the recording chamber was measured with a Clark-type oxygen electrode and decreased from approximately 610 mmHg P_{O_2} (hyperoxia) to 0.5 mmHg P_{O_2} (anoxia) within 5 min, which is the limit of detection for the P_{O_2} electrode and not different from that in the N_2/CO_2 bubbled reservoir. P_{O_2} levels were maintained at this level for the duration of anoxic experiments (data not shown).

Cell-attached 5–20 GΩ seals were obtained using the blind-patch technique described elsewhere (Blanton *et al.* 1989). Whole-cell recordings were performed using the voltage-clamp method with 5–8 MΩ borosilicate glass electrodes containing the following (mM): 8 NaCl, 0.0001 $CaCl_2$, 10 Na-Hepes, 20 KCl, 110 potassium gluconate, 1 $MgCl_2$, 0.3 NaGTP, 2 NaATP (adjusted to pH 7.4). Typical access resistance ranged from 10 to 30 MΩ and patches were discarded if access resistance changed by more than 20%. Data were collected using an Axopatch-1D amplifier, a CV-4 headstage, and a Tl-1 DMA interface (Axon Instruments, CA, USA) and then digitized and stored on computer using Clampex 6 software (Axon Instruments).

Normoxic experiments consisted of an O_2/CO_2 aCSF perfusion as described above. A fast-step perfusion system (VC-6 perfusion valve controller and SF-77B fast-step

perfusion system, Warner Instruments) was used to deliver 1 μM tetrodotoxin (TTX) and 300 μM NMDA. Prior to each recording cortical sheets were perfused with TTX for 5 min. Cells were then voltage clamped at −70 mV and NMDA was applied until a current was elicited (3–10 s, depending on the proximity of the perfusion system to the patched neuron). This NMDA application time was used for all recordings from the same neuron within a single experiment. The initial peak NMDA current was set to 100% and subsequent peak NMDA currents were normalized to this value. For anoxic and pharmacological experiments, NMDA was initially applied to cortical sheets in normoxic aCSF, and the evoked whole-cell current was set to 100% ($t = 0$ min). A second control NMDA current was obtained after 10 min and then cortical sheets were exposed to anoxic aCSF or aCSF containing specific receptor modulators for 40 min. NMDA evoked peak currents were monitored at 20 min intervals following the change in aCSF. Cells were then reperfused with control normoxic aCSF for 40 min and NMDA-evoked peak currents were monitored at 20 min intervals following reoxygenation.

Pharmacology

For whole-cell NMDAR experiments, cortical neurons were perfused with pharmacological modifiers in the bulk perfusate as specified in the Results. K_{ATP} channels were activated with levcromakalim (100 μM) or the mK_{ATP} channel-specific agonist diazoxide (10–350 μM) and blocked with glibenclamide (80 μM) or the mK_{ATP} channel-specific antagonist 5-hydroxydecanoic acid (5HD; 100 μM). Diazoxide is known to be 1000–2000 times more selectively potent for mK_{ATP} then for plasmalemmal K_{ATP} channels (pK_{ATP}) and is not an effective activator of pK_{ATP} channels at the concentrations used in this study ($K_{1/2}$: 855 μM) (Garlid *et al.* 1996, 1997). Furthermore, 5HD has little effect on pK_{ATP} channels but is a potent inhibitor of mK_{ATP} channel activity (McCullough *et al.* 1991; Garlid *et al.* 1997). Mitochondrial Ca^{2+}-sensitive K^+ (mK_{Ca}) channels were activated by NS-1619 (50 μM) and blocked by paxilline (1 μM) (Sato *et al.* 2005). A recording electrode solution containing 0 [ATP] was used to dialyse ATP from the cytosol as described elsewhere (Muller *et al.* 2002). To test the effect of succinate dehydrogenase (SDH) inhibition on NMDAR currents, malonate (5 mM) was bulk perfused (Sivaramakrishnan & Ramasarma, 1975). The potassium ionophore valinomycin (5 μM) and dinitrophenol (DNP; 10 mM) were used as positive controls for uncoupling experiments in isolated mitochondria (Knowles, 1982). For experiments involving Ca^{2+} chelation, 1,2-bis (*o*-aminophenoxy)ethane-*N*,*N*,*N*′,*N*′-tetraacetic acid (BAPTA, 5 mM) was included in the recording electrode solution (Shin *et al.* 2005). To modify ER Ca^{2+} release, thapsigargin (1 μM) and ryanodine (10 μM) were bath perfused to block the ER calcium ATPase and the ER ryanodine receptors, respectively. The mitochondrial Ca^{2+} uniporter was activated by spermine (500 μM) and blocked by ruthenium red (40 nM) (Allshire *et al.* 1985).

Immunohistochemistry

Turtle brains were dissected and incubated in aCSF containing a K_{ATP} channel-specific fluorophore (BODIPY-glibenclamide green, 500 nM), and a mitochondria-specific fluorophore (mitotracker deep red, 500 nM). Brains were incubated with the two flourophores for 90 min and then fixed for 48 h in 10% formaline and 30% sucrose at 4°C. Fixed brains were then frozen and the cortex was sliced using a cryostat to a thickness of 20 μm. Cortical slices were mounted on slides with Vectashield mounting medium (Vector Laboratories, CA, USA). Samples were imaged with a Zeiss LSM510 META Axioplan2 confocal microscope with ×4, ×40 and ×100 water-immersion lenses. Argon and helium neon lasers were used to excite the probes (ex/em): BODIPY-Green – 504/511; Mitotracker Deep Red – 644/655 nm. Data were analysed using Zeiss LSM410 software.

Assessment of cellular Ca^{2+} changes

Calcium changes were assessed using fura-2 excited at 380 nm. Basic methods for the dissection and loading of cortical sheets with fura-2 and measuring $[Ca^{2+}]_c$ changes are described elsewhere (Buck & Bickler, 1995). Briefly, cortical sheets were isolated as described for whole-cell patch clamp experiments and then preloaded with fura-2 in two consecutive 1 h incubations followed by a 15 min rinse in normal aCSF. Cortical sheets were incubated in the dark at 4°C and following dye loading were placed in a flow-through recording chamber equipped with the same perfusion system as the whole-cell patch clamp experiments. A custom cuff was placed around the objective to provide constant N_2 gas across the surface of the bath during anoxic exposure. Fura-2 was excited at 380 nm using a DeltaRam X high-speed random access monochromator and a LPS220B light source (PTI, NJ, USA). Fluorescence measurements were acquired at 1 min intervals using an Olympus BX51W1 microscope and U-CMAD3 camera (Olympus Canada Inc, Markham, ON, Canada). Baseline fluorescence was recorded for 10–20 min and then the tissue was exposed to treatment aCSF (as outlined in Results) for up to 40 min. Tissues were then reperfused with control aCSF. In another set of experiments tissues were exposed to rapid and repeated treatments. For each experiment 15 neurons were chosen at random and the average change in fura-2 fluorescence of these neurons was used for statistical comparison.

Isolation of mitochondria

Turtle heart mitochondria were used due to their abundance in this tissue relative to the comparatively lower abundance and mass of the turtle brain. Mitochondria respond similarly to mK_{ATP} channel modulation across a variety of tissues including brain, liver and heart (Holmuhamedov *et al.* 1998; Bajgar *et al.* 2001). For this reason we consider heart mitochondria to be an appropriate model in which to assess the response of turtle mitochondria to mK_{ATP} channel modulation. Detailed mitochondrial isolation procedures are reported elsewhere (Almeida-Val *et al.* 1994; Holmuhamedov, 1999). To minimize animal usage, hearts were obtained from those animals killed for cortical tissue. Briefly, mitochondria were suspended in an isolation solution consisting of (mM: 140 KCl, 20 Na-*N*-2-hydroxyethylpiperazine-*N*′-2-ethanesulphonic acid (Hepes), 10 EDTA, and 0.1% bovine serum albumin (BSA) adjusted to pH 7.20 at 20°C with KOH; osmolality 295–300 mosmol kg^{-1}). Mitochondrial pellets were suspended to approximately 1 mg mitochondrial protein per ml. Protein concentrations were analysed using a spectrophotometric bicinchoninic acid (BCA) endpoint protein assay calibrated to 37°C at a 562 nm using a Molecular Devices SpectraMax Plus plate spectrophotometer and SoftproMax® software.

Measurement of mitochondrial O_2 consumption

Rates of O_2 consumption were determined using a Clark-type oxygen electrode attached to a Gilson O_2 chamber. Mitochondria were suspended in incubation medium (mM: 140 KCl, 20 Hepes, 10 EDTA and 1 Na_2HPO_4) at a 1 : 8 ratio. Maximum respiratory control rates (RCRs) were achieved with 5 mM α-ketoglutarate (α-KG). State 2 rates were obtained before addition of ADP, state 3 rates after ADP and state 4 rates following consumption of ADP. The effects of pharmacological agents were assessed during state 2 or 4 respiration unless noted otherwise and drug concentrations were the same as those used during whole-cell recordings (see above). There was no significant difference between state 2 and 4 respiration for any drug treatment. Respiration rates were calculated using the LoggerPro v.2.2.1 software (Vernier, OR, USA). Electrodes were calibrated daily.

Chemicals

All chemicals were obtained from Sigma Chemical Co. (Oakville, ON, Canada). Diazoxide, thapsigargin, NS1619, levcromakalim, paxilline and glibenclamide were initially dissolved in dimethylsulphonic acid (DMSO), and then placed in aCSF not exceeding 1% v/v. Vehicle application alone did not affect NMDA evoked currents (data not shown). Fluorescent probes were obtained from Molecular Probes (Eugene, OR, USA).

Statistical Analysis

NMDAR whole-cell current data were analysed following root arcsine transformation using two-way ANOVA with a Student–Newman–Keuls (all pairwise) *post hoc* test to compare within and against treatment and normoxic values. Mitochondrial respiration data were analysed using Student's paired *t* test and one-way ANOVA. Significance was determined at $P < 0.05$, and all data are expressed as the mean ± standard error of mean (S.E.M.).

Results

ATP-sensitive K^+ channels are present in the cortex of the turtle

Turtle cortical sheets were stained using the live-cell fluorophores BODIPY-glibenclamide (K_{ATP} probe, Fig. 1*C* and *F*) and mitotracker deep red (mitochondrial probe, Fig. 1*D* and *G*). Pyramidal cells were visualized on a confocal microscope. Overlays of the two stains are shown in Fig. 1*E* and *H*. To our knowledge this is the first time that mK_{ATP} channels have been imaged in an intact brain slice.

Activation of mK_{ATP} mildly uncouples turtle mitochondria

K^+ channel openers increase mG_K, mildly uncoupling the mammalian mitochondrial inner membrane and accelerating O_2 respiration (Garlid *et al.* 1997). The effects of these drugs have not been previously studied in turtle mitochondria. We measured O_2 consumption as an indicator of mitochondrial activity and to evaluate the specificity of the pharmacological treatments used in the whole-cell experiments to mitochondrial ion channels. For mitochondrial experiments the average RCR was 10.8 ± 0.7. Administration of the vehicle (DMSO) alone had no effect on O_2 respiration rate (data not shown, $n = 5$). Activation of mK_{ATP} channels with levcromakalim (100 μM) or diazoxide (100 μM) increased O_2 respiratory rate 21.6 ± 4.0% and 88.6 ± 9.3%, respectively ($n = 6$ and 23, respectively, Fig. 2*A*, *B* and *E*). These effects were blocked by 100 μM 5HD ($n = 10$ for DZX + 5HD; $n = 5$ for LEV + 5HD, Fig. 2*C* and *F*).

The K^+ channel ionophore valinomycin (5 μM) was added to the mitochondrial preparation to artificially increase mG_K. Valinomycin addition resulted in a 413.9 ± 61.1% increase in respiration rate ($n = 8$, Fig. 2*D*). This increase was not blocked by 5HD (data not shown). Subsequent application of diazoxide to cells treated with valinomycin did not further increase respiration rate

($n = 6$, Fig. 2*D*). Since the effects of valinomycin and diazoxide were not additive, diazoxide and valinomycin were likely to have caused mitochondrial uncoupling via a similar mechanism, which is increased mG_K. NS1619 (50 μM), which opens another mitochondrial K^+ channel (the Ca^{2+}-sensitive K^+ channel: mK_{Ca}), was applied to further examine the role of increased mG_K in uncoupling mitochondria. NS1619 increased the respiration rate by $73.8 \pm 13.9\%$ ($n = 6$, Fig. 2*G*). As a positive control, complete uncoupling of the mitochondria with the protonophore dinitrophenol (DNP; 10 mM) resulted in a $760.2 \pm 135.1\%$ increase in respiration rate (data not shown, $n = 8$). If DNP is considered to completely uncouple mitochondrial respiration then the uncoupling effect of mK_{ATP} channel activation with diazoxide is about 9.7% of the overall rate of O_2 consumption.

The rate of mitochondrial ATP production was used as a second measure of mitochondrial uncoupling. ADP was added to isolated mitochondria to initiate state 3 respiration and the sample was allowed to respire until state 4 respiration was achieved. Once a new steady state had been reached, diazoxide was added to the mitochondria to open mK_{ATP} channels and a second amount of ADP was added to the mitochondria (Fig. 3*A*). Results were compared to double ADP addition experiments without the addition of diazoxide between substrate additions. In mitochondria with diazoxide, oxygen consumption rates decreased by $22.6 \pm 1.6\%$ while the time required for the mitochondria to utilize the available ADP for ATP production increased by $50.4 \pm 20.5\%$ ($n = 9$, Fig. 3*B*).

Mitochondrial uncoupling via activation of K^+ channels regulates $[Ca^{2+}]_c$ during normoxia and anoxia

A small elevation of $[Ca^{2+}]_c$ is central to the anoxic attenuation of turtle NMDAR activity, but its source is not known (Bickler *et al.* 2000; Shin *et al.* 2005). Mitochondrial Ca^{2+} uptake occurs primarily via the mitochondrial Ca^{2+} uniporter, which is driven by the electrochemical gradient across the mitochondrial inner membrane. Therefore, uncoupling of mitochondria should impair mitochondrial Ca^{2+} handling by reducing the driving force on the uniporter. Since mitochondria are major Ca^{2+} buffers in the cell, decreases in mitochondrial Ca^{2+} uptake should cause elevations in $[Ca^{2+}]_c$. In turtle cortical slices $[Ca^{2+}]_c$ did not change during normoxia, but increased during anoxic perfusion by $9.4 \pm 0.3\%$ ($n = 5, 7$, Fig. 4*A–C*). This effect was reversed by reperfusion with normoxic aCSF. The anoxic increase in $[Ca^{2+}]_c$ was blocked by 5HD ($n = 4$, Figs 4*A* and *E*). Furthermore, normoxic perfusion of diazoxide or levcromakalim induced elevations in $[Ca^{2+}]_c$ of $8.9 \pm 0.7\%$ and $3.8 \pm 0.3\%$, respectively ($n = 3$ for each, Figs 4*A*, *F* and *H*). These increases were reversed by drug

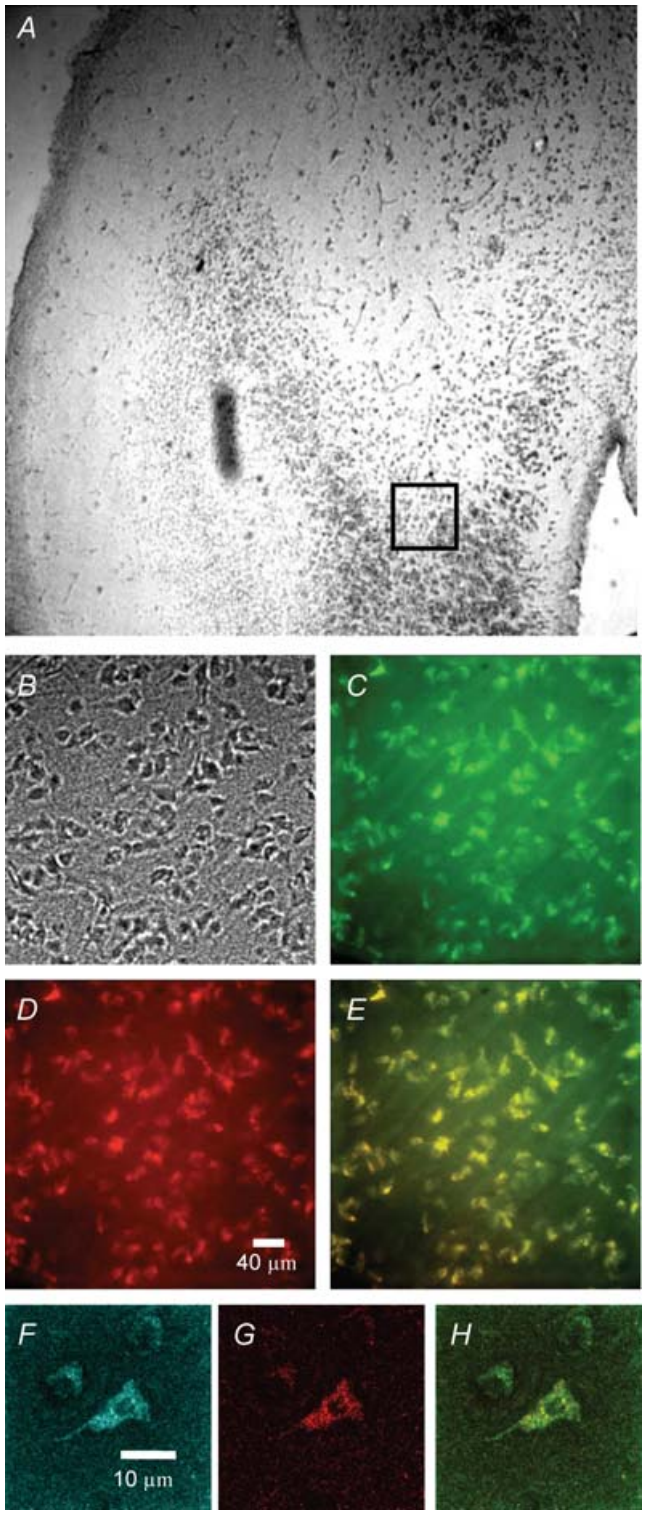

Figure 1. K_{ATP} channels in the turtle cortex
A, turtle cortical sheet (4× magnification). *B–E*, boxed region in *A* at 40× magnification. (F-H) are a single neuron at 100× magnification. *B*, a bright field image of the cortical sheet. (*C* and *F*, BODIPY-glibenclamide staining to visualize K_{ATP} channels *D* and *G*, MitoTracker Deep Red to stain mitochondria. Images were overlaid to show colocalization between mitochondria and mK_{ATP} channels (*E* and *H*).

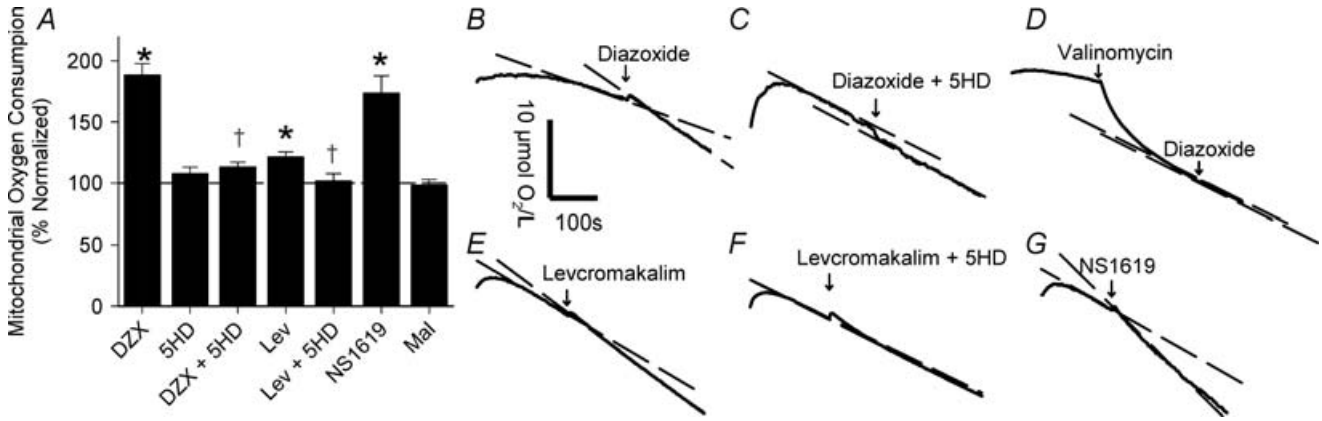

Figure 2. Effects of K_{ATP} activation on the state 2 or 4 rate of mitochondrial oxygen consumption
A, percentage normalized mitochondrial respiration rates following treatment. Dashed line represents control rate of oxygen consumption before drug application. Symbols indicate data significantly different from normoxic controls (*) or drug treatment controls (†). Data are expressed as means ± S.E.M. *B–G*, sample oxygen consumption curves. Arrows indicate the addition of pharmacological treatments to state 2 respiring mitochondria. Dotted lines represent the slopes used to determine changes in rate before and after treatment. Abbreviations: diazoxide (DZX), levcromakalim (Lev), malonate (Mal), 5-hydroxydecanoic acid (5HD).

washout and prevented by simultaneous perfusion with 5HD ($n = 3$ for each, Figs 4*A*, *G* and *I*). To determine if the source of the $[Ca^{2+}]_c$ was intra- or extracellular, slices were perfused with anoxic aCSF with 0 $[Ca^{2+}]$ and 5 mM EGTA. In these experiments anoxia resulted in an increase in $[Ca^{2+}]_c$ of 10.5 ± 0.7%, indicating the source of the anoxic elevation of $[Ca^{2+}]_c$ is cellular and not due to Ca^{2+} entry from extracellular sources ($n = 4$, Figs 4*A* and *D*).

Mitochondrial and not plasmalemmal K^+ channel opening modifies NMDAR activity

We examined the role of both mitochondrial and plasmalemmal K_{ATP} and mK_{Ca} channels in regulating NMDAR activity using whole-cell voltage-clamp recordings from turtle cortical pyramidal neurons. During 50 min of normoxic perfusion turtle NMDAR currents did not change, but decreased 48.9 ± 4.1 and

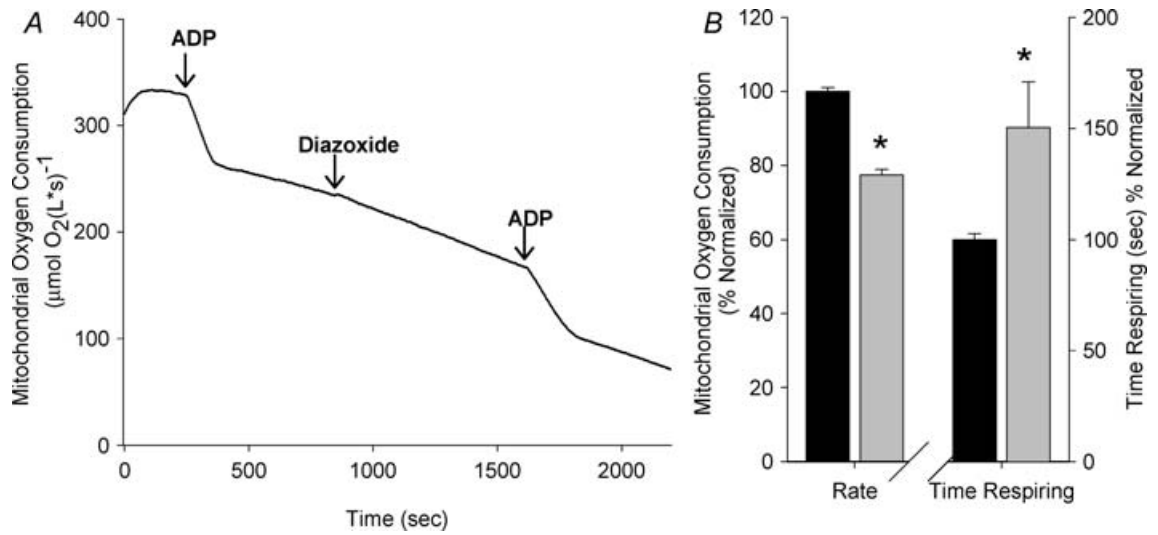

Figure 3. Change in the rate of ATP production with mK_{ATP} channel-mediated mitochondrial uncoupling
A, a representative experiment. Arrows indicate addition of substrate (ADP) or diazoxide. The resulting change in rate and the time before respiration returns to baseline was measured and compared to experiments without diazoxide addition. *B*, graph showing mean changes in oxygen consumption rates and total state 3 respiration time. Black bar represents control without diazoxide, grey bar represents oxygen consumption with diazoxide. Asterisks indicates data significantly different from control values. Data are presented as means ± S.E.M.

$54 \pm 5.2\%$ at 30 and 50 min of anoxia, respectively ($n = 10$ for each, Fig. 5*A*, *C* and *D*). During normoxia, activation of mK_{ATP} channels with the general K_{ATP} channel agonist levcromakalim decreased whole-cell NMDAR currents 39.4 ± 3.1 and $49.7 \pm 6.7\%$ at 30 and 50 min, respectively ($n = 9$, Fig. 5*A* and *E*). The mK_{ATP}-specific agonist diazoxide (350 μM) resulted in a similar decrease in NMDAR activity of 43.8 ± 10.0 and $41.1 \pm 6.7\%$ at 30 and 50 min, respectively ($n = 7$, Fig. 5*A* and *F*). Similar results were seen at lower concentrations of diazoxide (100 μM), which decreased NMDAR currents $40.5 \pm 10\%$ after 50 min perfusion ($n = 10$, Fig. 5*B*). At 10 μM, diazoxide had no effect on NMDAR currents ($n = 4$). The diazoxide-mediated decreases were not statistically different from the anoxic decrease in NMDAR activity ($P > 0.001$). The effect of both levcromakalim and diazoxide was abolished by perfusion of glibenclamide or the mK_{ATP} channel-specific antagonist 5HD ($n = 8$ and 6, respectively, Fig. 5*A* and *G*). During anoxia, the decrease in NMDAR currents was abolished by mK_{ATP} channel blockade with glibenclamide or 5HD ($n = 10$ and 8, respectively, Fig. 5*A*, *H* and *I*).

SDH inhibition by diazoxide

Diazoxide can also inhibit SDH activity at high concentrations (Schafer *et al.* 1969; Busija *et al.* 2005). To determine whether SDH inhibition decreased NMDAR activity, the effect of the specific SDH inhibitor malonate on NMDAR activity was examined. Perfusion of 5 mM malonate during normoxic recording did not alter NMDAR activity ($n = 7$, Fig. 5*J*). In another experiment, cells were initially exposed to malonate and subsequently to diazoxide. In these experiments malonate had no effect on NMDAR currents but diazoxide application reduced normoxic NMDAR currents by $47.1 \pm 16.1\%$ ($n = 5$, Fig. 5*A*). As an additional control, isolated mitochondria were perfused with malonate. Malonate did not significantly change mitochondrial respiration rate in either state 2 or state 4 ($n = 6$), but significantly decreased

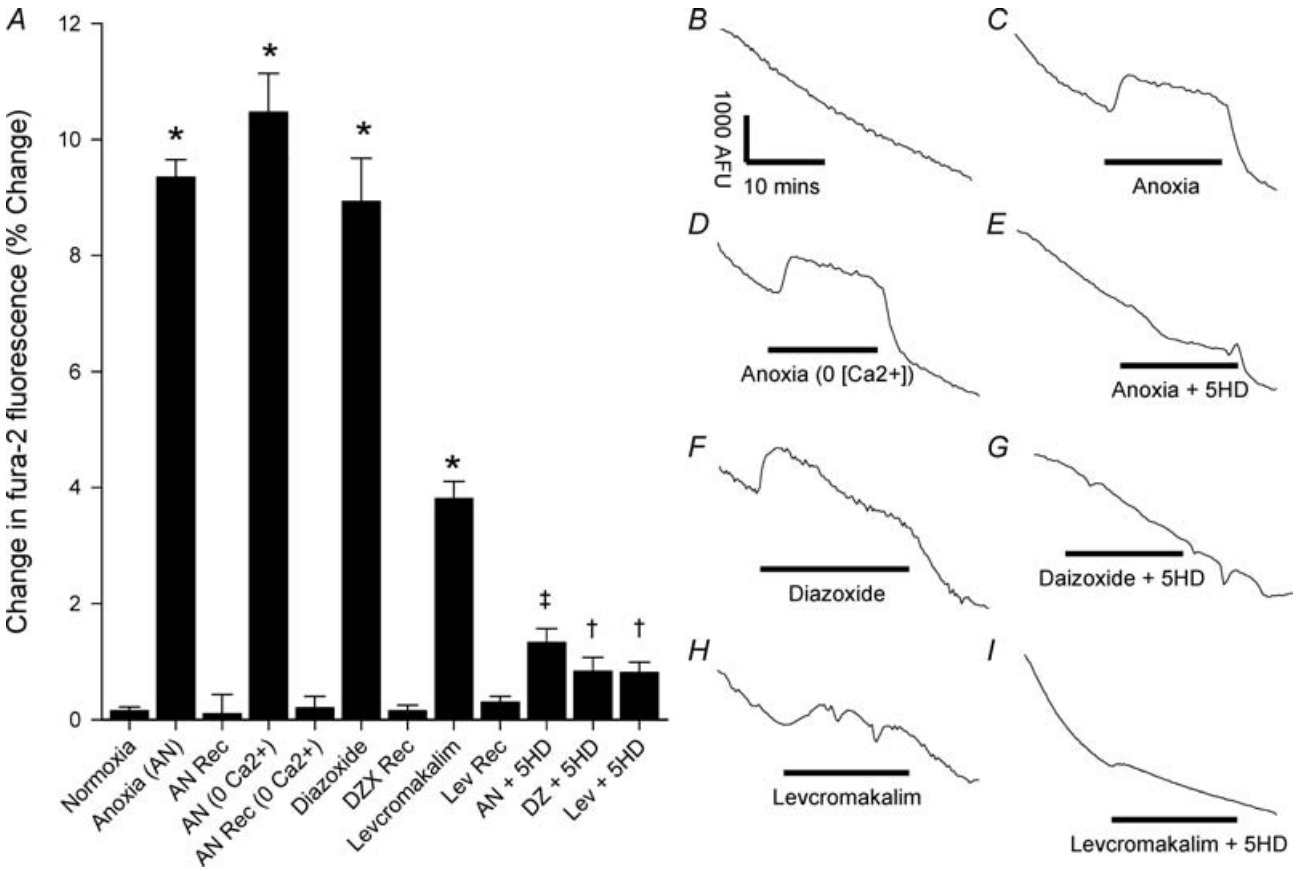

Figure 4. Change in fura-2 $[Ca^{2+}]_c$ fluorescence during anoxia and following mitochondrial uncoupling
A, percentage normalized changes in fura-2 calcium fluorescence at 1 min post treatment. Symbols indicate data significantly different from normoxic control (*), anoxic control (‡), or drug treatment control (†). Data are expressed as means ± S.E.M. *B–I*, raw data traces of fura-2 calcium fluorescence from neurons treated as indicated. AFU, arbitrary fluorescence units. Abbreviations: diazoxide (DZX), levcromakalim (Lev), anoxia (AN), 5-hydroxydecanoic acid (5HD).

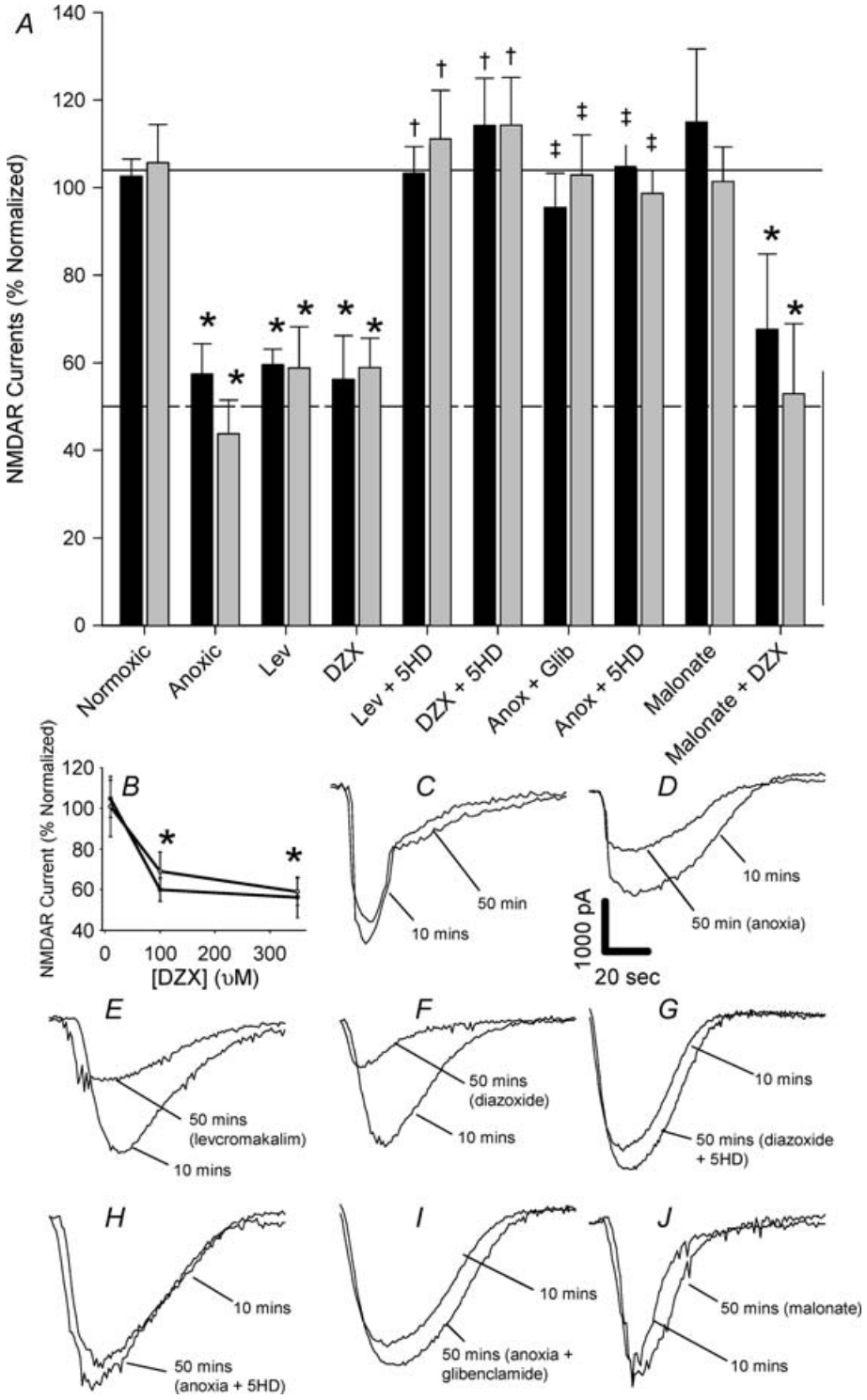

Figure 5. Effect of K^+ channel openers on whole-cell NMDAR currents
A, percentage normalized NMDAR currents at $t = 30$ min (black bars) and 50 min (grey bars) of treatment. Continuous line represents normoxic controls, dashed line represents anoxic controls. *B*, dose–response curve of normalized paired normoxic NMDAR currents *versus* [diazoxide]. Symbols indicate data significantly different from normoxic control (*), anoxic control (‡), or drug treatment control (†). Data are expressed as means ± S.E.M. *C–I*, paired sample NMDAR currents at $t = 10$ min (control) and following 40 min of treatment exposure ($t = 50$ min). Abbreviations: diazoxide (DZX), levcromakalim (Lev), glibenclamide (Glib), 5-hydroxydecanoic acid (5HD), anoxia (anox).

the rate of O_2 consumption by $74.8 \pm 8.1\%$ in state 3 mitochondria ($n = 10$, data not shown). Diazoxide also decreased state 3 respiration rates by $37.3 \pm 2.1\%$ ($n = 7$, data not shown) and this decrease was not blocked by 5HD ($n = 5$, data not shown). Taken together, these data suggest that the inhibition of SDH by diazoxide occurs primarily during state 3 respiration and does not affect the regulation of coupled mitochondria.

Plasmalemmal ATP-sensitive K^+ channels

To examine the role of pK_{ATP} channels on NMDAR currents, we dialysed ATP out of the cytosol to a nominal concentration using patch electrodes filled with ISCF containing 0 [ATP]. Over the course of several hours (data shown up to 50 min), ATP dialysis did not alter NMDAR activity during normoxic perfusion, nor did it affect the anoxic-mediated decrease in NMDAR activity ($n = 7$ and 8, respectively, Fig. 6). Importantly, application of diazoxide to ATP-dialysed cells resulted in a decrease in NMDAR activity of $40.8 \pm 6.2\%$ ($n = 6$, Fig. 6). This decrease was statistically similar to the pharmacological activation of mK_{ATP} channels at normal $[ATP]_c$.

The role of increased K^+ conductance

To confirm that the mK_{ATP} channel-mediated decrease of NMDAR activity was due to a change in mG_K, we studied the effect of mK_{Ca} channel modulation on normoxic NMDAR activity. Activation of these channels increased mG_K in a similar fashion to mK_{ATP} channel activation. Administration of the mK_{Ca} channel agonist NS1619 caused a decrease in NMDAR activity of 51.7 ± 8.4 and $50.0 \pm 6.5\%$ at 30 and 50 min of NS1619 perfusion, respectively, similar to mK_{ATP} channel activation ($n = 11$, Fig. 7). The mK_{Ca} channel-mediated decrease in NMDAR currents was blocked by the K_{Ca} channel antagonist paxilline (1 μM), but not by mK_{ATP} channel blockade with 5HD ($n = 4$ and 3, respectively, Fig. 7*A*). In addition, the mK_{ATP} channel-mediated decrease in NMDAR activity was not prevented by mK_{Ca} channel blockade with paxilline ($n = 3$, Fig. 7). To confirm the role of K^+ channels in this response, a set of experiments were performed using the general K^+ channel blocker caesium (1.2 mM). Caesium perfusion had no effect on normoxic NMDAR activity, but did prevent the anoxic decrease in whole-cell NMDAR currents supporting the hypothesis that increased mG_K underlies the anoxic regulation of NMDAR activity ($n = 7$ and 8, respectively, Fig. 7).

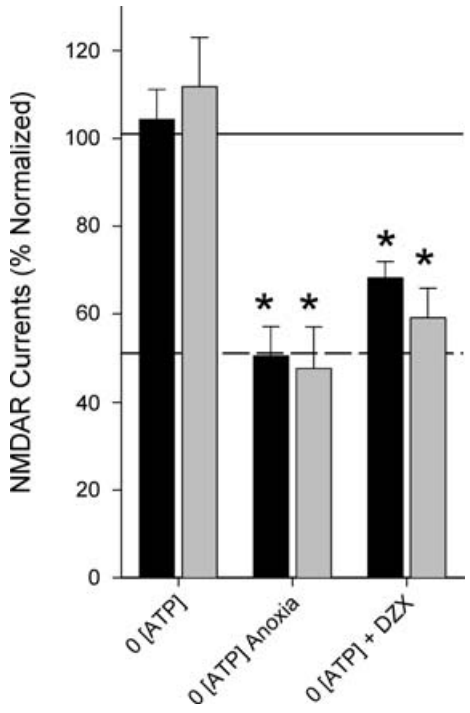

Figure 6. Role of $[ATP]_c$ and pK_{ATP} channels on whole-cell NMDAR currents
Percentage normalized NMDAR currents at $t = 30$ min (black bars) and 50 min (grey bars) of treatment. Continuous line represents normoxic controls, dashed line represents anoxic controls. Symbols indicate data significantly different from normoxic controls. Data are expressed as means ± S.E.M. Experiments are normoxic except where indicated. Abbreviations: diazoxide (DZX).

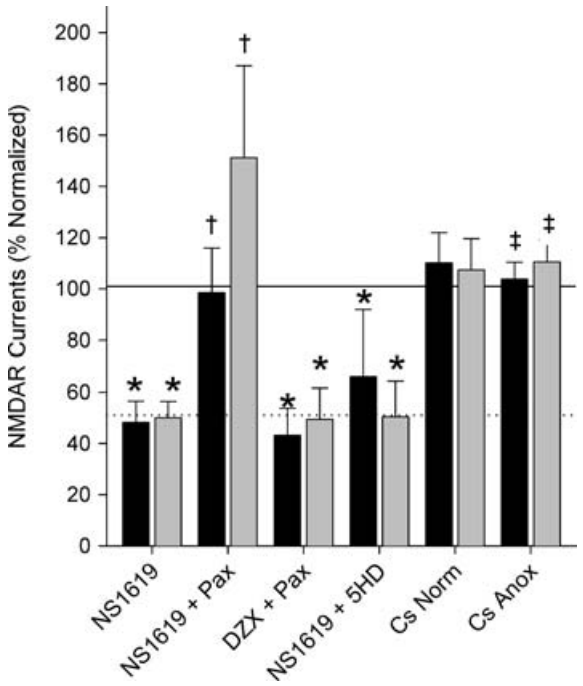

Figure 7. Effect of increased mitochondrial potassium conductance on whole-cell NMDAR currents
Percentage normalized NMDAR currents at $t = 30$ min (black bars) and 50 min (grey bars) of treatment. Continuous line represents normoxic controls, dashed line represents anoxic controls. Symbols indicate data significantly different from normoxic control (*), anoxic control (‡), or drug treatment control (†). Data are expressed as means ± S.E.M. Abbreviations: diazoxide (DZX), paxallin (Pax), caesium (Cs) normoxia (norm), anoxia (anox).

Intracellular Ca^{2+} sources

Chelation of $[Ca^{2+}]_c$ with 5 mM BAPTA prevented the anoxic decrease in NMDAR currents, confirming that the anoxic decrease in NMDAR activity is mediated by Ca^{2+} ($n = 8$, Fig. 8). The primary cellular sources of Ca^{2+} are the endoplasmic reticulum (ER) and mitochondria. To examine the role of Ca^{2+} from ER stores in NMDAR regulation, ER Ca^{2+} release was blocked by inhibiting the ryanodine receptor (with 10 μM ryanodine, $n = 7$) or the ER Ca^{2+}-ATPase (ERCA; with 1 μM thapsigargin, $n = 10$). In both cases, inhibition had no effect on normoxic NMDAR currents. Furthermore, this blockade did not prevent the anoxic decrease in NMDAR activity ($n = 3$ for each). To determine if mitochondrial uncoupling affects normoxic NMDAR activity by Ca^{2+} modulation, diazoxide was coapplied in the presence of BAPTA. Chelation of $[Ca^{2+}]_c$ prevented the diazoxide-mediated decrease of normoxic NMDAR currents ($n = 8$, Fig. 8), implicating mitochondrial Ca^{2+} handling as a regulatory link between anoxic activation of mK_{ATP} channels and subsequent reductions in NMDAR activity.

mK_{ATP} channel-mediated decreases in NMDAR currents are regulated via the activity of the Ca^{2+} uniporter

Mitochondrial uncoupling inhibits the Ca^{2+} uniporter and direct blockade of the uniporter with 40 nM ruthenium red resulted in a decrease in normoxic NMDAR currents of 44.4 ± 5.3 and 47.1 ± 9.1% at 30 and 50 min, respectively ($n = 7$, Fig. 9). This decrease was blocked by BAPTA but not by 5HD, indicating the decrease is Ca^{2+} mediated and downstream of mK_{ATP} channel activation ($n = 6$ for each, Fig. 9). Spermine (500 μM) is a known activator of the mitochondrial Ca^{2+} uniporter. Perfusion of this polyamine had no effect on peak normoxic NMDAR currents but abolished the anoxic and diazoxide-mediated decreases in NMDAR activity ($n = 5$ for each, Fig. 9).

Spermine is both an activator of the mitochondrial Ca^{2+} uniporter (Sparagna *et al.* 1995; Zhang *et al.* 2006) and, at higher concentrations, a potentiator of NMDAR currents (Takano *et al.* 2005). To ensure that spermine was not involved in NMDAR potentiation, we performed normoxic control experiments with 500 μM and 2.5 mM spermine. At the lower concentration we found no significant potentiation of NMDAR activity (Fig. 9). At the higher concentration, only 2 out of 9 recorded neurons showed potentiation (data not shown). Since potentiation was rarely seen, even at higher spermine concentrations, we can exclude the possibility that spermine directly potentiated NMDAR activity in our experiments.

Discussion

mK_{ATP} channels regulate $[Ca^{2+}]_c$ and NMDARs via 'mild uncoupling' of mitochondria

We proposed that in the turtle brain, mild mitochondrial uncoupling leads to changes in Ca^{2+} homeostasis and alters NMDAR function. Indeed, we demonstrate that mitochondrial uncoupling by the opening of mK_{ATP} channels with diazoxide increases $[Ca^{2+}]_c$ and decreases NMDAR currents during normoxia. Similarly, during anoxia $[Ca^{2+}]_c$ increases and NMDAR currents are reduced. The diazoxide or anoxia-mediated changes were blocked by the inclusion of the mK_{ATP} channel blockers 5HD and glibenclamide. Opening of mK_{ATP} channels uncouples mitochondria by increasing mG_K (Fig. 10). This specificity of action was confirmed by increasing

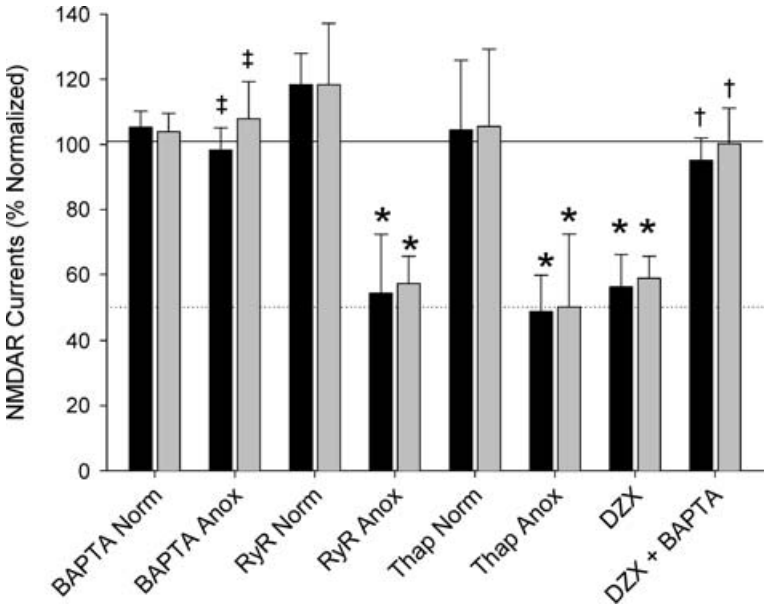

Figure 8. Role of cellular Ca^{2+} modulators on whole-cell NMDAR currents
Percentage normalized NMDAR currents at $t = 30$ min (black bars) and 50 min (grey bars) of treatment. Continuous line represents normoxic controls, dashed line represents anoxic controls. Symbols indicate data significantly different from normoxic control (*), anoxic control (‡), or drug treatment control (†). Data are expressed as means ± S.E.M. Abbreviations: ryanodine (RyR), thapsigargin (Thap)., diazoxide (DZX), normoxia (norm), anoxia (anox).

mG_K independently of mK_{ATP}: activation of mK_{Ca} also decreased normoxic NMDAR currents, mimicking the effects of mK_{ATP} channel activation or anoxia. Blocking mK_{Ca} during anoxic perfusion did not abolish the decrease in NMDAR activity, however, confirming the specific action of mK_{ATP} channels on the anoxic regulation of NMDARs.

In isolated mitochondria, mK_{ATP} channel activation caused mild uncoupling. Increased O_2 consumption rates and decreases in ATP production following diazoxide addition indicate mK_{ATP} channel activation uncouples turtle mitochondria by 10–20%. These measurements are similar to the 12–14% uncoupling of mitochondrial membrane potential observed with similar drug application in mammalian mitochondria (Holmuhamedov, 1998; Murata *et al.* 2001). Furthermore, the effects of diazoxide and valinomycin on mitochondrial respiration rate were not cumulative: valinomycin induced maximum mG_K and diazoxide had no additional effect on mitochondria already partially uncoupled by valinomycin. This suggests that the uncoupling action of diazoxide occurs via an increase in K^+ conductance.

The regulatory link between mK_{ATP} channel-mediated 'mild uncoupling' and NMDARs is a decrease in mitochondrial Ca^{2+} uniporter activity. Mitochondrial uncoupling dissipates the H^+ electrochemical gradient that drives the activity of this pump, reducing Ca^{2+} uptake into the mitochondria (Fig. 10). Therefore, blockade of the uniporter with ruthenium red mimics the effect of uncoupling on mitochondrial Ca^{2+} uptake. Mitochondria are a major calcium sink in the cell, and thus a decrease in mitochondrial Ca^{2+} uptake results in an elevation of $[Ca^{2+}]_c$. In our experiments, antagonism of the uniporter reduced normoxic NMDAR currents similarly to anoxia and diazoxide or levcromakalim application. Secondly, chelation of $[Ca^{2+}]_c$ abolished the anoxia-, diazoxide- and ruthenium red-mediated decreases in NMDAR activity. Finally, activation of the uniporter abolished both the anoxia- and diazoxide-mediated decreases in NMDAR currents. Together these data indicate mK_{ATP} channels uncouple mitochondria, reducing the activity of the uniporter, limiting mitochondrial Ca^{2+} uptake, subsequently elevating $[Ca^{2+}]_c$ and decreasing NMDAR activity.

Anoxic turtle NMDAR regulation and mammalian ischaemic preconditioning are mediated by similar mechanisms

In mammalian neurons, ischaemic insults cause complete depolarization of the mitochondrial membrane potential and formation of mitochondrial permeability transition pores (MPTPs), which are associated with the release of apoptotic activators and cell death. Ischaemic preconditioning (IPC) causes mK_{ATP} channels to open, inducing a mild uncoupling of the mitochondrial membrane potential, which leads to neuroprotective effects including prevention of further mitochondrial depolarization, MPTP formation and cell death (Ishida *et al.* 2001; Murata, 2001).

Although the exact mechanisms that underlie this neuroprotection remain unidentified, many aspects of the pathway have been elucidated and are remarkably similar to the mechanism of NMDAR arrest in turtle brain identified here. In mammals, IPC induces mK_{ATP} channel-mediated mitochondrial uncoupling, which prevents mitochondrial Ca^{2+} overload by limiting Ca^{2+} uptake via the mitochondrial Ca^{2+} uniporter (Holmuhamedov, 1998; Rousou *et al.* 2004; Saotome *et al.* 2005) and by activating cyclosporin-sensitive Ca^{2+} release from the mitochondria (Holmuhamedov, 1999). In rat hearts exposed to ischaemia, $[Ca^{2+}]_c$ was elevated 4-fold while mitochondrial calcium ($[Ca^{2+}]_m$) rose 10-fold and tissue death ensued. Treatment with diazoxide caused further elevation of $[Ca^{2+}]_c$ by ~50%, but $[Ca^{2+}]_m$ elevation was reduced by 80% and survival

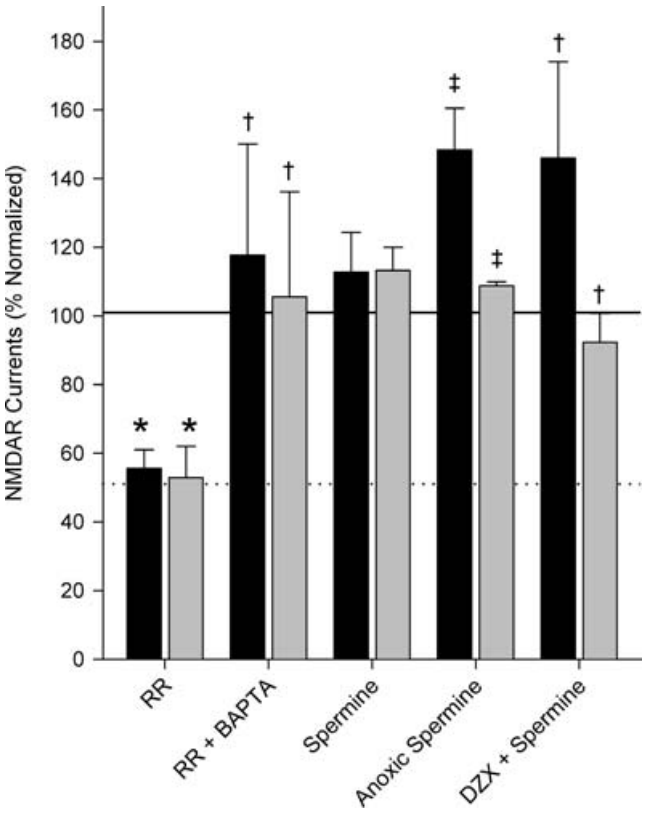

Figure 9. Role of the mitochondrial Ca^{2+}-uniporter on whole-cell NMDAR currents
Percentage normalized NMDAR currents at $t = 30$ min (black bars) and 50 min (grey bars) of treatment. Continuous line represents normoxic controls, dashed line represents anoxic controls Symbols indicate data significantly different from normoxic control (*), anoxic control (‡), or drug treatment control (†). Data are expressed as mean ± S.E.M. Abbreviations: diazoxide (DZX), ruthenium red (RR).

was improved (Wang *et al.* 2001). These authors concluded that ischaemia-induced elevations in $[Ca^{2+}]_m$ are toxic in rats and that lowering $[Ca^{2+}]_m$ overload is an underlying protective mechanism in IPC. In another study ruthenium red was used to block mitochondrial Ca^{2+} uptake via the uniporter. Just as ruthenium red mimicked anoxia-mediated NMDAR decrease in the turtle, it also mimics the protective effects of IPC in rat hearts: reducing infarct size, lactate dehydrogenase (LDH) leakage and mitochondria permeability transition pore (MPTP) formation. Furthermore, activation of the mitochondrial Ca^{2+} uniporter with spermine prevented IPC-mediated cardio-protection and induced MPTP formation (Zhang *et al.* 2006). Thus activation of mK_{ATP} channels during ischaemia compromises uniporter activity and prevents toxic elevation of $[Ca^{2+}]_m$.

Although the importance of preventing mitochondrial calcium accumulation has been demonstrated, a potential link between mK_{ATP} channels and NMDARs has received little attention. One study found that diazoxide enhanced glutamatergic currents in hippocampal neurons (Crepel *et al.* 1993). However, these changes were likely to have been due to secondary effects of diazoxide on succinate dehydrogenase activity since these authors used a high concentration of diazoxide (600 μM), and their findings were neither blocked by the K_{ATP} channel antagonists glibenclamide or tolbutamide, nor mimicked by other K_{ATP} channel agonists such as galanine. A few studies have indicated a potential protective mechanism involving mK_{ATP} channels and NMDARs. In rat hippocampal cultures ECD was prevented when neurons were treated with K^+ channel activators, preventing Ca^{2+} fluctuations. This protection was reversed by glyburide, a general K_{ATP} channel antagonist (Abele & Miller, 1990). One study of interest demonstrated that inhibition of mitochondrial Ca^{2+} uptake desensitized NMDAR activity (Kannurpatti, 2000). While this study did not involve K_{ATP} channels, it demonstrated a link between mitochondrial Ca^{2+} handling and NMDAR function.

Plasmalemmal *versus* mitochondrial KATP channels

Our results suggest that mitochondrial, and not plasmalemmal, K_{ATP} channels mediate changes in

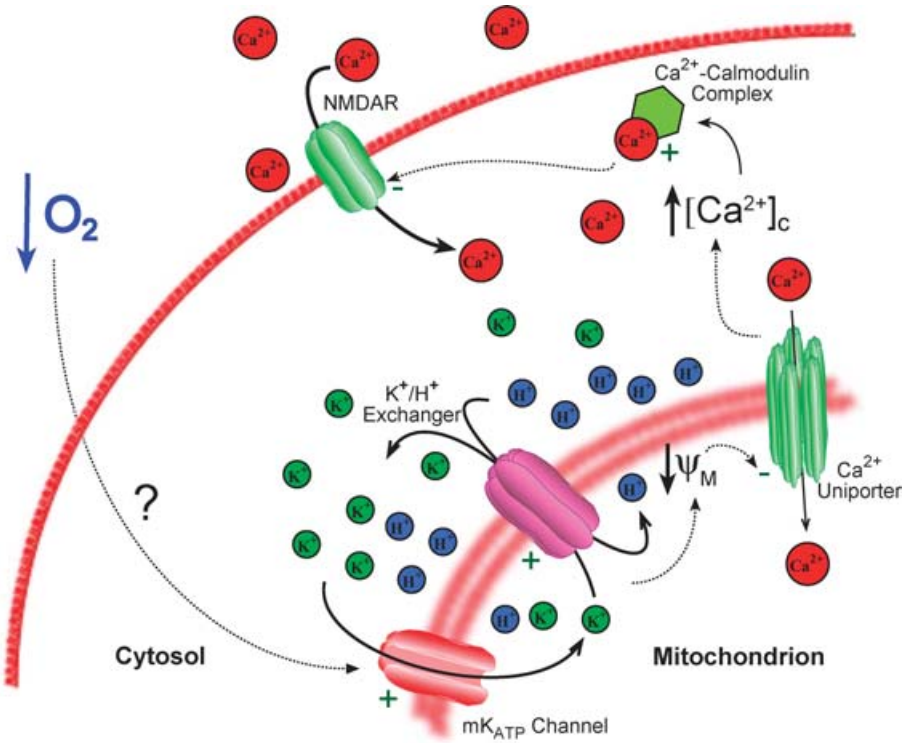

Figure 10. Schematic depicting a proposed mechanism of mK_{ATP} channel-mediated NMDA receptor channel arrest
Dotted lines represent direction of pathway progression in a counter-clockwise direction commencing with decreased oxygen availability. The signal via which oxygen availability is transmitted to the mitochondria is unknown. During anoxia, increased opening of mK_{ATP} channels augments K^+ efflux from the mitochondria. Increased K^+ efflux leads to futile K^+/H^+ cycling and mildly decreases the mitochondrial membrane potential (Ψ_M). This mild uncoupling reduces the driving force on the mitochondrial Ca^{2+} uniporter, slowing mitochondrial Ca^{2+} uptake and subsequently raising $[Ca^{2+}]_c$. Mildly elevated $[Ca^{2+}]_c$ complexes with calmodulin and decreases the influx of ions through the NMDAR via a mechanism also involving protein kinases and phosphatases; see Shin *et al.* (2005).

NMDAR activity. K_{ATP} channels are activated by decreases in [ATP] on the inside of the membrane the channel is spanning. Thus plasmalemmal (pK_{ATP}) and mK_{ATP} channels are regulated by changes in cytosolic and mitochondrial [ATP], respectively (Zhang *et al.* 2001; Matsuo *et al.* 2005). Even though neuronal $[ATP]_c$ decreases 23% with anoxia in the turtle (Buck *et al.* 1998), it is unlikely that pK_{ATP} channels are involved in NMDAR regulation because ATP dialysis did not alter NMDAR activity during either normoxic or anoxic perfusion, nor did it prevent the effect of diazoxide application on NMDAR activity. These results, combined with the actions of the specific mitochondrial K_{ATP} channel modulators (diazoxide and 5HD) on whole-cell NMDAR currents and $[Ca^{2+}]_c$, provide evidence that mitochondrial and not plasmalemmal K_{ATP} channels regulate NMDAR during anoxia. It should be noted that the anoxic decrease in $[ATP]_c$ in turtle cortex may have limited effects on the activity of pK_{ATP} channels. The cytosol is compartmentalized, particularly near the plasma membrane and the activity of ATP-dependent channels is related to change in adenylate concentrations in these membrane localized subcompartments and not necessarily to $[ATP]_c$ as a whole (Babenko *et al.* 1998).

K_{ATP} channels in the anoxic turtle brain

Glibenclamide binding density studies indicate K_{ATP} channels are distributed throughout the turtle brain (Jiang *et al.* 1992); however, research into their role in the anoxia tolerance of turtle brain is sparse and conflicting. For example, Jiang *et al.* (1992) reported that K_{ATP} channel blockade with glibenclamide had no effect on anoxic K^+ efflux, but others have reported that K_{ATP} blockade reduces K^+ efflux during early anoxia (Pek-Scott & Lutz, 1998). These authors blocked K_{ATP} channels with glibenclamide in the first hour and with 2,3-butanedione monoxime (BDM) during 2–4 h of anoxia. Unfortunately, the use of BDM limits the conclusions that can be drawn from these data regarding the role of K_{ATP} channels. In brain, BDM has been shown to inhibit L-type calcium channels and glycine-gated chloride currents and to increase GABAergic currents (Allen *et al.* 1998; Brightman *et al.* 1995; Ye & McArdle 1996). More importantly regarding K^+ currents, BDM has been shown to directly regulate K^+ flux via inhibition of Kv2.1 channels (Lopatin & Nichols, 1993).

There is evidence that K_{ATP} activation may decrease glutamate release and maintain dopamine release in the anoxic turtle cortex (Milton & Lutz, 1998; Milton *et al.* 2002; Thompson *et al.* 2007). While experiments with diazoxide in those studies offer some support for a role of mK_{ATP} channels in the normoxic regulation of dopamine and glutamate release, conclusions regarding the role of K_{ATP} channels in the anoxic regulation of these metabolites is also based on treatment of cells with BDM.

NMDAR depression and anoxic survival in the turtle cortex

The western painted turtle survives for months without oxygen at 3°C and days at 25°C (Musacchia, 1959; Ultsch & Jackson, 1982). This survival is mediated by a wide variety of mechanisms that are up-regulated at various stages of hypoxia, anoxia and reoxygenation (for a review see Milton & Prentice, 2007). Interestingly, blockade of any single mechanism is not deleterious to the animal. Thus its remarkable anoxic tolerance is likely to be due to the combination of this mosaic of protective mechanisms. NMDAR depression is one mechanism that appears to function throughout the duration of anoxic exposure. $[Ca^{2+}]_c$ is mildly elevated and NMDAR activity is decreased within 20 min of anoxic perfusion, and during prolonged anoxia (6 weeks) $[Ca^{2+}]_c$ remains slightly elevated and the decrease in NMDAR activity is maintained (Bickler & Buck, 1998). Over the same time period, extracellular $[Ca^{2+}]$ increases 6-fold, highlighting the importance of NMDAR down-regulation to prevent toxic intracellular calcium accumulation. Conversely, in rats $[Ca^{2+}]_c$ becomes elevated 10-fold within minutes of anoxia and this Ca^{2+} influx is entirely mediated by NMDARs (Bickler & Hansen, 1994).

In addition to a direct reduction in NMDAR activity, the turtle employs a variety of other mechanisms to further suppress NMDAR-mediated calcium entry. During prolonged anoxia NMDARs are removed from the plasma membrane and glutamate release is decreased (Bickler *et al.* 2000; Thompson *et al.* 2007). Furthermore, recent studies in our lab indicate that the activity of a second glutamate receptor, the α-amino-3-hydroxy-5-methylisoxazole-4-propionic acid receptor (AMPAR), also undergoes channel arrest during anoxia (Pamenter *et al.* 2007). AMPARs function upstream of NMDARs and their activation removes the voltage-dependent Mg^{2+} plug from the NMDAR. Taken together, these data suggests an emphasis on reduced excitatory signalling in the turtle brain that is predicated on glutamate receptor channel arrest.

The turtle's survival is enhanced by low temperatures experienced during hibernation, likely to be mediated by Q_{10}-related reductions in metabolic rate and not temperature-dependent regulation of NMDARs. Hypothermia does not protect against NMDA-mediated neurotoxicity in mammals and NMDAR currents are not affected by changes in temperature (Bickler *et al.* 1994; Takadera & Ohyashiki, 2007). Therefore, our model of decreased NMDAR activity would likely apply across all temperature ranges experienced by the turtle during anoxia (Bickler *et al.* 1994).

In conclusion, our study provides evidence that mK_{ATP} channel activation uncouples turtle mitochondria and subsequently decreases NMDAR activity. Mitochondrial

uncoupling decreases Ca^{2+} uptake via the mitochondrial uniporter, raising cytosolic calcium levels and decreasing both normoxic and anoxic NMDAR currents (Fig. 10). mK_{ATP} channels are currently considered a primary mediator of IPC-mediated protection, but the end-mediators of this protection are undetermined in mammals. To our knowledge, this is the first study that demonstrates mK_{ATP} channel regulation of NMDARs and may represent a common mechanism between the prevention of excitotoxic cell death and preconditioned neuroprotection from ischaemic insult.

References

Abele AE & Miller RJ (1990). Potassium channel activators abolish excitotoxicity in cultured hippocampal pyramidal neurons. *Neurosci Lett* **115**, 195–200.

Allen TJ, Mikala G, Wu X & Dolphin AC (1998). Effects of 2,3-butanedione monoxime (BDM) on calcium channels expressed in *Xenopus* oocytes. *J Physiol* **508**, 1–14.

Allshire A, Bernardi P & Saris NE (1985). Manganese stimulates calcium flux through the mitochondrial uniporter. *Biochim Biophys Acta* **807**, 202–209.

Almeida-Val VM, Buck LT & Hochachka PW (1994). Substrate and acute temperature effects on turtle heart and liver mitochondria. *Am J Physiol Regul Integr Comp Physiol* **266**, R858–R862.

Arundine M & Tymianski M (2003). Molecular mechanisms of calcium-dependent neurodegeneration in excitotoxicity. *Cell Calcium* **34**, 325–337.

Babenko AP, Aguilar-Bryan L & Bryan J (1998). A view of sur/KIR6.X, K_{ATP} channels. *Annu Rev Physiol* **60**, 667–687.

Bajgar R, Seetharaman S, Kowalowski AJ, Garlid KD & Paucek P (2001). Identification and properties of a novel intracellular (mitochondrial) ATP-sensitive potassium channel in brain. *J Biol Chem* **276**, 33369–33374.

Bickler PE & Buck LT (1998). Adaptations of vertebrate neurons to hypoxia and anoxia: maintaining critical Ca^{2+} concentrations. *J Exp Biol* **201**, 1141–1152.

Bickler PE, Buck LT & Hansen BM (1994). Effects of isoflurane and hypothermia on glutamate receptor-mediated calcium influx in brain slices. *Anesthesiology* **81**, 1461–1469.

Bickler PE, Donohoe PH & Buck LT (2000). Hypoxia-induced silencing of NMDA receptors in turtle neurons. *J Neurosci* **20**, 3522–3528.

Bickler PE & Fahlman CS (2004). Moderate increases in intracellular calcium activate neuroprotective signals in hippocampal neurons. *Neuroscience* **127**, 673–683.

Bickler PE & Hansen BM (1994). Causes of calcium accumulation in rat cortical brain slices during hypoxia and ischemia: role of ion channels and membrane damage. *Brain Res* **665**, 269–276.

Blanton MG, Lo Turco JJ & Kriegstein AR (1989). Whole cell recording from neurons in slices of reptilian and mammalian cerebral cortex. *J Neurosci Methods* **30**, 203–210.

Brightman T, Ye JH, Ortiz-Jimenez E, Flynn EJ, Wu WH & McArdle JJ (1995). 2,3-Butanedione monoxime protects mice against the convulsant effect of picrotoxin by facilitating GABA-activated currents. *Brain Res* **678**, 110–116.

Buck LT & Bickler P (1995). Role of adenosine in NMDA receptor modulation in the cerebral cortex of an anoxia-tolerant turtle (*Chrysemys picta belli*). *J Exp Biol* **198**, 1621–1628.

Buck LT & Bickler P (1998). Adenosine and anoxia reduce N-methyl-D-aspartate receptor open probability in turtle cerebrocortex. *J Exp Biol* **201**, 289–297.

Buck L, Espanol M, Litt L & Bickler P (1998). Reversible decreases in ATP and PCr concentrations in anoxic turtle brain. *Comp Biochem Physiol A Mol Integr Physiol* **120**, 633–639.

Buck LT & Pamenter ME (2006). Adaptive responses of vertebrate neurons to anoxia – Matching supply to demand. *Respir Physiol Neurobiol* **154**, 226–240.

Busija DW, Katakam P, Rajapakse NC, Kis B, Grover G, Domoki F & Bari F (2005). Effects of ATP-sensitive potassium channel activators diazoxide and BMS-191095 on membrane potential and reactive oxygen species production in isolated piglet mitochondria. *Brain Res Bull* **66**, 85–90.

Choi DW (1992). Excitotoxic cell death. *J Neurobiol* **23**, 1261–1276.

Crepel V, Rovira C & Ben-Ari Y (1993). The K^+ channel opener diazoxide enhances glutamatergic currents and reduces GABAergic currents in hippocampal neurons. *J Neurophysiol* **69**, 494–503.

Garlid KD, Paucek P, Yarov-Yarovoy V, Murray HN, Darbenzio RB, D'Alonzo AJ, Lodge NJ, Smith MA & Grover GJ (1997). Cardioprotective effect of diazoxide and its interaction with mitochondrial ATP-sensitive K^+ channels. Possible mechanism of cardioprotection. *Circ Res* **81**, 1072–1082.

Garlid KD, Paucek P, Yarov-Yarovoy V, Sun X & Schindler PA (1996). The mitochondrial K_{ATP} channel as a receptor for potassium channel openers. *J Biol Chem* **271**, 8796–8799.

Heurteaux C, Lauritzen I, Widmann C & Lazdunski M (1995). Essential role of adenosine, adenosine A1 receptors, and ATP-sensitive K^+ channels in cerebral ischemic preconditioning. *Proc Natl Acad Sci U S A* **92**, 4666–4670.

Holmuhamedov EL, Jovanovic S, Dzeja PP, Jovanovic A & Terzic A (1998). Mitochondrial ATP-sensitive K^+ channels modulate cardiac mitochondrial function. *Am J Physiol Heart Circ Physiol* **44**, H1567–H1576.

Holmuhamedov EL, Wang L & Terzic A (1999). ATP-sensitive K^+ channel openers prevent Ca^{2+} overload in rat cardiac mitochondria. *J Physiol* **519**, 347–360.

Ikonomidou C & Turski L (2002). Why did NMDA receptor antagonists fail clinical trials for stroke and traumatic brain injury? *Lancet Neurol* **1**, 383–386.

Ishida H, Hirota Y, Genka C, Nakazawa H, Nakaya H & Sato T (2001). Opening of mitochondrial K_{ATP} channels attenuates the ouabain-induced calcium overload in mitochondria. *Am J Physiol Heart Circ Physiol* **89**, 856–858.

Jiang C, Xia Y & Haddad GG (1992). Role of ATP-sensitive K^+ channels during anoxia: major differences between rat (newborn and adult) and turtle neurons. *J Physiol* **448**, 599–612.

Kannurpatti SS, Joshi PG & Joshi NB (2000). Calcium sequestering ability of mitochondria modulates influx of calcium through glutamte receptor channel. *Neurochem Res* **25**, 1527–1536.

Kis B, Nagy K, Snipes JA, Rajapakse NC, Horiguchi T, Grover GJ & Busija DW (2004). The mitochondrial K_{ATP} channel opener BMS-191095 induces neuronal preconditioning. *Neuroreport* **15**, 345–349.

Kis B, Rajapakse NC, Snipes JA, Nagy K, Horiguchi T & Busija DW (2003). Diazoxide induces delayed pre-conditioning in cultured rat cortical neurons. *J Neurochem* **87**, 969–980.

Knowles AF (1982). Differential effects of 2,4-dinitrophenol and valinomycin (+ K^+) on uncoupler-stimulated ATPase of human tumor mitochondria. *Biochim Biophys Acta* **681**, 62–71.

Lopatin AN & Nichols CG (1993). 2,3-Butanedione monoxime (BDM) inhibition of delayed rectifier DRK1 (Kv2.1) potassium channels expressed in *Xenopus oocytes*. *J Pharmacol Exp Ther* **265**, 1011–1016.

Matsuo M, Kimura Y & Ueda K (2005). K_{ATP} channel interaction with adenine nucleotides. *J Mol Cell Cardiol* **38**, 907–916.

McCullough JR, Normandin DE, Conder ML, Sleph PG, Dzwonczyk S & Grover GJ (1991). Specific block of the anti-ischemic actions of cromakalim by sodium 5-hydroxydecanoate. *Circ Res* **69**, 949–958.

Milton SL & Lutz PL (1998). Low extracellular dopamine levels are maintained in the anoxic turtle (*Trachemys scripta*) striatum. *J Cereb Blood Flow Metab* **18**, 803–807.

Milton SL & Prentice HM (2007). Beyond anoxia: the physiology of metabolic downregulation and recovery in the anoxia-tolerant turtle. *Comp Biochem Physiol A Mol Integr Physiol* **147**, 277–290.

Milton SL, Thompson JW & Lutz PL (2002). Mechanisms for maintaining extracellular glutamate levels in the anoxic turtle striatum. *Am J Physiol Regul Integr Comp Physiol* **282**, R1317–R1323.

Muller M, Brockhaus J & Ballanyi K (2002). ATP-independent anoxic activation of ATP-sensitive K^+ channels in dorsal vagal neurons of juvenile mice in situ. *Neuroscience* **109**, 313–328.

Murata M, Akao M, O'Rourke B & Marban E (2001). Miochondrial ATP-sensitive potassium channels attenuate matrix Ca^{2+} overload during stimulated ischemia and reperfusion. *Circulation Res* **89**, 891–898.

Murry CE, Jennings RB & Reimer KA (1986). Preconditioning with ischemia: a delay of lethal cell injury in ischemic myocardium. *Circulation* **74**, 1124–1136.

Musacchia XJ (1959). The viability of *Chrysemys picta* submerged at various temperatures. *Physiol Zoo* **1**, 57–50.

Pamenter ME, Shin DS & Buck LT (2007). AMPA receptors undergo channel arrest in the anoxic turtle cortex. *Am J Physiol Regul Integr Comp Physiol* (in press).

Pek-Scott M & Lutz PL (1998). ATP-sensitive K^+ channel activation provides transient protection to the anoxic turtle brain. *Am J Physiol Regul Integr Comp Physiol* **275**, R2023–R2027.

Rousou AJ, Ericsson M, Federman M, Levitsky S & McCully JD (2004). Opening of mitochondrial K_{ATP} channels enhances cardioprotection through the modulation of mitochondrial matrix volume, calcium accumulation, and respiration. *Am J Physiol Heart Circ Physiol* **287**, H1967–H1976.

Saotome M, Katoh H, Satoh H, Nagasaka S, Yoshihara S, Terada H & Hayashi H (2005). Mitochondrial membrane potential modulates regulation of mitochondrial Ca^{2+} in rat ventricular myocytes. *Am J Physiol Heart Circ Physiol* **288**, H1820–H1828.

Sato T, Saito T, Saegusa N & Nakaya H (2005). Mitochondrial Ca^{2+}-activated K^+ channels in cardiac myocytes: a mechanism of the cardioprotective effect and modulation by protein kinase A. *Circulation* **111**, 198–203.

Schafer G, Wegener C, Portenhauser R & Bojanovski D (1969). Diazoxide, an inhibitor of succinate oxidation. *Biochem Pharmacol* **18**, 2678–2681.

Semenov DG, Samoilov Zielonka MO & Lazarewiscz P (2000). Responses to reversible anoxia of intracellular free and bound Ca^{2+} in rat cortical slices. *Resuscitation* **44**, 207–214.

Shimizu K, Lacza Z, Rajapakse N, Horiguchi T, Snipes J & Busija DW (2002). MitoK_{ATP} opener, diazoxide, reduces neuronal damage after middle cerebral artery occlusion in the rat. *Am J Physiol Heart Circ Physiol* **283**, H1005–H1011.

Shin DS & Buck LT (2003). Effect of anoxia and pharmacological anoxia on whole-cell NMDA receptor currents in cortical neurons from the western painted turtle. *Physiol Biochem Zool* **76**, 41–51.

Shin DS, Wilkie MP, Pamenter ME & Buck LT (2005). Calcium and protein phosphatase 1/2A attenuate N-methyl-D-aspartate receptor activity in the anoxic turtle cortex. *Comp Biochem Physiol A Mol Integr Physiol* **142**, 50–57.

Sivaramakrishnan S & Ramasarma T (1975). Oxidation of succinate in heart, brain, and kidney mitochondria in hypobaria and hypoxia. *Environ Physiol Biochem* **5**, 189–200.

Sparagna GC, Gunter KK, Sheu SS & Gunter TE (1995). Mitochondrial calcium uptake from physiological-type pulses of calcium. A description of the rapid uptake mode. *J Biol Chem* **270**, 27510–27515.

Takadera T & Ohyashiki T (2007). Temperature-dependent N-methyl-D-aspartate receptor-mediated cytotoxicity in cultured rat cortical neurons. *Neurosci Lett* **423**, 24–28.

Takano K, Ogura M, Nakamura Y & Yoneda Y (2005). Neuronal and glial responses to polyamines in the ischemic brain. *Curr Neurovasc Res* **2**, 213–223.

Thompson JW, Prentice HM & Lutz PL (2007). Regulation of extracellular glutamate levels in the long-term anoxic turtle striatum: coordinated activity of glutamate transporters, adenosine, $K^+{}_{ATP}$ channels and GABA. *J Biomed Sci* **14**, 809–817.

Ultsch GR & Jackson DC (1982). Long-term submergence at 3 degrees C of the turtle *Chrysemys picta bellii* in normoxic and severely hypoxic water. III. Effects of changes in ambient P_{O2} and subsequent air breathing. *J Exp Biol* **97**, 87–99.

Wang L, Cherednichenko G, Hernandez L, Halow J, Camacho SA, Figueredo V & Schaefer S (2001). Preconditioning limits mitochondrial Ca^{2+} during ischemia in rat hearts: role of K_{ATP} channels. *Am J Physiol Heart Circ Physiol* **280**, H2321–H2328.

Ye JH & McArdle JJ (1996). 2,3-Butanedione monoxime modifies the glycine-gated chloride current of acutely isolated murine hypothalamic neurons. *Brain Res* **735**, 20–29.

Zhang DX, Chen YF, Campbell WB, Zou AP, Gross GJ & Li PL (2001). Characteristics and superoxide-induced activation of reconstituted myocardial mitochondrial ATP-sensitive potassium channels. *Circ Res* **89**, 1177–1183.

Zhang SZ, Gao Q, Cao CM, Bruce IC & Xia Q (2006). Involvement of the mitochondrial calcium uniporter in cardioprotection by ischemic preconditioning. *Life Sci* **78**, 738–745.

Zipfel GJ, Babcock DJ, Lee JM & Choi DW (2000). Neuronal apoptosis after CNS injury: the roles of glutamate and calcium. *J Neurotrauma* **17**, 857–869.

Acknowledgements

We would like to thank Joe Hayek, Alex Tonkikh and Henry Hong for their assistance with the confocal imaging and sample preparation, and Dr Chris Moyes for the use of the mitochondrial respiratory apparatus. This research was supported by a National Science and Engineering Research Council (NSERC) of Canada grant, a Premiers Research Excellence Award (PREA) and an Ontario Graduate Scholarship in Science and Technology (OGGST).